

## Inferring Fall Attitudes of Pristine Dendritic Crystals from Polarimetric Radar Data

SERGEY Y. MATROSOV

*Cooperative Institute for Research in Environmental Sciences, University of Colorado, and NOAA/Environmental Technology Laboratory, Boulder, Colorado*

ROGER F. REINKING AND IRINA V. DJALALOVA

*Science and Technology Corp., and NOAA/Environmental Technology Laboratory, Boulder, Colorado*

(Manuscript received 21 October 2003, in final form 30 June 2004)

### ABSTRACT

Single pristine planar ice crystals exhibit some flutter around their preferential horizontal orientation as they fall. This study presents estimates of flutter and analyzes predominant fall attitudes of pristine dendritic crystals observed with a polarization agile  $K_a$ -band cloud radar. The observations were made in weakly precipitating winter clouds on slopes of Mt. Washington, New Hampshire. The radar is capable of measuring the linear depolarization ratios in the standard horizontal-vertical polarization basis (HLDR) and the slant  $45^\circ$ – $135^\circ$  polarization basis (SLDR). Both HLDR and SLDR depend on crystal shape. HLDR also exhibits a strong dependence on crystal orientation, while SLDR depends only weakly on orientation. The different sensitivities of SLDR and HLDR to the shape and orientation effects are interpreted to estimate the angular flutter of crystals. A simple analytical expression is derived for the standard deviation of angular flutter as a function of the HLDR to SLDR ratio assuming perfect radar system characteristics. The flutter is also assessed by matching theoretical and observed depolarization patterns as a function of the elevation of the radar's beam. The matching procedure is generally more robust since it accounts for the actual polarization states and imperfections in the radar hardware. The depolarization approach was used to estimate flutter of falling pristine dendrites that were characterized by Reynolds numbers in a range of approximately 40–100. Using the matching approach, this flutter was found to be about  $9^\circ \pm 3^\circ$ , as expressed by the standard deviation of the crystal minor axes from the vertical direction. The analytical expression provides a value of flutter of about  $12^\circ$ , which is at the high end of the estimate obtained by the matching procedure. The difference is explained by the imperfections in the polarization states and radar hardware, so the analytical result serves as an upper bound to the more robust result from matching. The values of flutter estimated from the experimental example are comparable to estimates for planar crystals obtained in laboratory models and by individual crystal sampling.

### 1. Introduction

In the absence of electric field forces, symmetrical planar ice crystals with Reynolds numbers in the range  $1 < N_{Re} < 100$  tend to fall with their major dimensions oriented preferentially in the horizontal plane with very small flutter. Eddies formed at the rear of symmetrical crystals begin to shed, and secondary motions including glide-pitch oscillations and spiral motions (“flutter”) are introduced at  $N_{Re} \geq 100$  (Pruppacher and Klett 1997). In contrast, many natural planar crystals have some asymmetry and begin to exhibit secondary motions if  $N_{Re} \geq 40$  (Kajikawa 1992). Single dendrites are

often characterized by such values of  $N_{Re}$ , which is defined as

$$N_{Re} = VD/\nu, \quad (1)$$

where  $V$  is the fall velocity of a planar crystal with diameter  $D$ , and  $\nu$  is the kinematic viscosity of the air. Using photographs of light pillars (i.e., the optical phenomenon caused by horizontally oriented crystals), Sassen (1980) confirmed that planar crystals flutter around their preferred horizontal orientation. He concluded that the angular deviation from the horizontal orientation of these crystals is Gaussian in character and one of the factors in crystal flutter is turbulent air motions, which, like trailing eddies, also displace the crystals from their initial orientations.

Reliable knowledge of the falling attitudes of atmospheric ice crystals is important for a number of atmospheric research areas. In lidar remote sensing, oriented ice crystals cause the effect of specular reflection at the

---

*Corresponding author address:* Dr. Sergey Y. Matrosov, CIRES, University of Colorado, and NOAA/Environmental Technology Laboratory, 325 Broadway, R/ET7, Boulder, CO 80305.  
E-mail: sergey.matrosov@noaa.gov

zenith direction (e.g., Platt 1978). Also, orientations of particles in ice clouds need to be known for correct estimation of cloud radiative effects. Kajikawa (1992) pointed out that crystal flutter could significantly affect physical cloud and precipitation processes involving hydrometeor collisions, thus influencing crystal riming and aggregation.

The depolarization measurements conducted by scanning polarization-agile cloud radars offer a unique new way for estimations of ice crystal falling attitudes. This study presents an approach for estimating the standard deviation of the planar crystal axes of rotation from the vertical, which is the parameter that quantitatively describes particle flutter. Hereafter, the axis that is perpendicular to the basic plane of a planar crystal is defined as the crystal rotation axis. This approach is based on depolarization measurements. It is applicable to the stratiform situations when one hydrometeor planar habit dominates radar returns, which happens in weakly precipitating snow clouds with dendritic crystals. This situation is more common in winter boundary layer clouds. Middle and high level clouds are often dominated by irregular nonpristine shape particles (e.g., Korolev et al. 2000), which do not exhibit clear polarization patterns in radar returns.

The experimental data were obtained with the National Oceanic and Atmospheric Administration's (NOAA) Environmental Technology Laboratory (ETL)  $K_a$ -band radar. The measurements were made in weakly precipitating winter storm events observed during the Mount Washington Icing Sensors Program (MWISP) in New Hampshire (Ryerson et al. 2000). This radar employs a quasi-optical technology for changing and selecting the polarization state of transmitted signals by rotating a phase-retarding plate (PRP) in front of the transmitter (Matrosov and Kropfli 1993). Co- and cross-polar component radar returns are measured simultaneously. A PRP with a phase shift of about  $177.4^\circ$  (a perfect half-wave plate with  $180^\circ$  phase shift was unavailable) was utilized for MWISP. Positioning this PRP with its axis in the horizontal plane provides measurements of horizontal linear depolarization ratio (HLDR), and rotating the PRP to  $22.5^\circ$  with respect to the horizontal offers measurements of a quasi-slant- $45^\circ$  linear depolarization ratio (SLDR) (Matrosov et al. 2001; Reinking et al. 2002). Both HLDR and SLDR are sensitive to particle apparent shape and orientation, but in different ways. The differences provide a means to quantitatively estimate the degree of particle flutter.

## 2. Depolarization ratios

A simple geometric shape that enables the modeling of radar depolarization ratios is that of a spheroid. Radar wavelengths are usually much greater than single dendrite sizes. Under this condition, their scattering

properties depend largely on their overall shape and not on small differences in particle structure (Dungey and Bohren 1993). This overall shape is defined by the aspect ratio  $r$ , which represents the ratio of particle minor and major dimensions. It was demonstrated (Matrosov et al. 1996, 2001) that the spheroidal shape with an appropriate assumption about hydrometeor aspect ratio and density is suitable for modeling depolarization properties at radar frequencies.

For an individual planar particle modeled as an oblate spheroid with the absence of propagation effects, the depolarization ratios are proportional to the ratios of terms containing squares of the nondiagonal and diagonal scattering matrix elements (e.g., Matrosov 1991):

$$S_{\text{LDR}} \propto |(S_{hh} - S_{vv}) \sin(\pi/4 - \alpha) \cos(\pi/4 - \alpha)|^2 \\ |S_{hh} \cos^2(\pi/4 - \alpha) + S_{vv} \sin^2(\pi/4 - \alpha)|^{-2}, \quad (2a)$$

$$H_{\text{LDR}} \propto |(S_{hh} - S_{vv}) \sin\alpha \cos\alpha|^2 \\ |S_{hh} \cos^2\alpha + S_{vv} \sin^2\alpha|^{-2}, \quad (2b)$$

where  $S_{hh}$  and  $S_{vv}$  are the backscattering amplitudes in the particle projection onto the radar polarization plane and  $\alpha$  is the canting angle, which is the angle between the projection of the particle axis of rotation onto the radar polarization plane and the vector of the vertical polarization. Figure 1 shows the relation of the canting angle with other angles characterizing the particle orientation. In this figure, the XYZ and X'Y'Z' coordinate systems define the particle orientation with respect to the horizontal plane and to the incident radar beam,

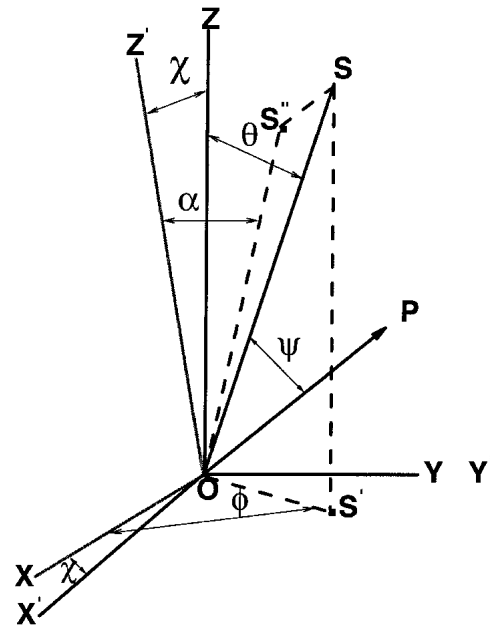


FIG. 1. Geometry of scattering.

correspondingly. The vector OS is along the particle rotation axis, and OS'' and OS' are its projections onto the radar polarization (i.e., Y'OZ') and horizontal (i.e., XOY) planes, respectively. Angle  $\chi$  is the radar elevation angle, and  $\theta$  and  $\phi$  are the particle rotation axis zenith and azimuth polar angles, respectively.

It can be easily shown that (2a) can be also written as

$$S_{\text{LDR}} \propto |(S_{hh} - S_{vv}) \cos 2\alpha|^2$$

$$|S_{hh} + S_{vv} + (S_{hh} - S_{vv}) \sin 2\alpha|^{-2}. \quad (2c)$$

For small flutter and low radar elevation angle,  $S_{vv}$  and  $S_{hh}$  are very close to the principal scattering amplitudes along the crystal rotation axis,  $S_v$ , and along the crystal major dimension,  $S_h$ , (e.g., Matrosov 1991):

$$S_{vv} \approx S_v, \quad (3a)$$

$$S_{hh} \approx S_h. \quad (3b)$$

For mixtures of ice and air that make up the volume occupied by a dendrite crystal, the imaginary parts of the complex refractive index  $m$  are very small compared to their real parts (Matrosov 1992). Since the amplitudes  $S_v$  and  $S_h$  in the Rayleigh regime are proportional to the product involving terms containing  $m^2$  and the imaginary unity  $j$  (Bohren and Huffman 1983), these amplitudes can be treated as pure imaginary numbers rather than complex numbers. Figure 2 shows the geometrical aspect ratio (i.e., the ratio of the crystal thickness along its rotation axis to its major dimension) and the backscattering amplitude ratio  $|S_h|/|S_v|$  as a function of the dendrite diameter  $D$  (i.e., the major dimension). The calculation procedure is outlined in detail by Matrosov (1991). The following assumptions about the thickness of the dendrite crystal,  $h$  (note that the aspect ratio is defined by  $h/D$ ), and its bulk density

$\rho$  were applied in the calculations (Pruppacher and Klett 1997):

$$h(\text{cm}) = 0.00902 D^{0.377} (\text{cm}), \quad (4)$$

$$\rho(\text{g cm}^{-3}) = 0.588 D^{-0.38} (\text{mm}) \quad (D > 0.3 \text{ mm}). \quad (5)$$

Changes in bulk density result in changes of the refractive index of the particle medium with size. This effect is responsible for the local maximum in  $|S_h|/|S_v|$  near  $D = 0.3 \text{ mm}$ —the diameter beyond which the bulk density of a dendrite starts diminishing (Fig. 2). For the case of a constant bulk density of solid ice, the ratio  $|S_h|/|S_v|$  would approach a value of  $m^2$  ( $m \approx 1.78$  for solid ice) as the geometrical aspect ratio decreases.

Hereafter, a distinction is made between depolarization ratios expressed in traditional decibel scale (i.e., SLDR and HLDR) and in linear units ( $S_{\text{LDR}}$  and  $H_{\text{LDR}}$ ):

$$\text{HLDR}(\text{dB}) = 10 \log_{10}(H_{\text{LDR}}),$$

$$\text{SLDR}(\text{dB}) = 10 \log_{10}(S_{\text{LDR}}). \quad (6)$$

Orientation dependence of  $H_{\text{LDR}}$  and  $S_{\text{LDR}}$  is introduced primarily through  $\alpha$ . For  $\alpha = 0$ , theoretically  $H_{\text{LDR}} = 0$ . In practice,  $H_{\text{LDR}}$  never reaches 0 due to polarization “cross talk” between the two polarimetric components. For the NOAA Ka-band radar, this cross talk amounts to about 0.0003 (i.e.,  $\sim -35 \text{ dB}$ ). For small values of  $\alpha$  (small flutter), one can derive from (2) the following expression for the ratio  $H_{\text{LDR}}/S_{\text{LDR}}$ :

$$H_{\text{LDR}}/S_{\text{LDR}} \approx 4\alpha^2 k(\alpha), \quad (7)$$

where  $k(\alpha)$  is a coefficient that depends on  $\alpha$  only relatively weakly:

$$k(\alpha) = |S_{hh} \cos^2(\pi/4 - \alpha) + S_{vv} \sin^2(\pi/4 - \alpha)|^2$$

$$|S_{hh} \cos^2 \alpha + S_{vv} \sin^2 \alpha|^{-2}. \quad (8)$$

It is assumed hereafter that all angular quantities are in radians unless degrees are specifically mentioned. For dendrites with typical diameters from 500  $\mu\text{m}$  to 2 mm viewed at low radar elevation angles,  $S_{hh} \approx 1.8 S_{vv}$  (see Fig. 2). Given this fact, it can be shown that the mean value of  $k(\alpha) \approx 0.69 \pm 0.09$  if  $|\alpha| < 0.2$ , and the ratio (7) can be approximated as

$$H_{\text{LDR}}/S_{\text{LDR}} \approx 2.8 \alpha^2. \quad (9)$$

The dendrite orientation in space is defined by two polar angles: the zenith angle  $\theta$  and the azimuth angle  $\phi$  of the dendrite axis of rotation. As mentioned above, the angle distribution with respect to  $\theta$  can be assumed to be normal (i.e., Gaussian), and the distribution of dendrite axis projections in the horizontal plane (i.e., the distribution of the axis of rotation with respect to the azimuth angle  $\phi$ ) is assumed to be random. From the general equations relating radar elevation angle  $\chi$ , canting angle  $\alpha$ , the zenith angle  $\theta$ , and the azimuth

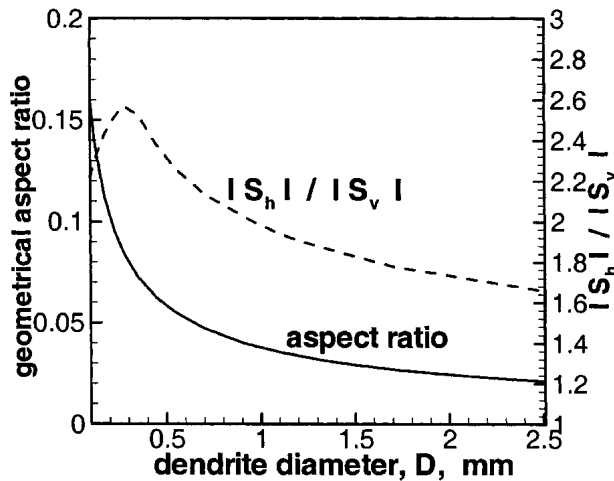


FIG. 2. Geometrical aspect ratio and the principal axes backscattering amplitude ratio for simple pristine dendrites as a function of the dendrite diameter.

angle  $\varphi$  (Holt 1984), the following relation can be obtained for small values of  $\chi$  and small flutter:

$$\alpha \approx \theta \sin \varphi. \quad (10)$$

Using (10), the mean absolute value of the canting angle  $\langle |\alpha| \rangle$  can be approximately expressed in terms of the mean absolute value of the crystal zenith angle  $\langle |\theta| \rangle$ :

$$\langle |\alpha| \rangle \approx \langle |\theta| \rangle (2/\pi). \quad (11)$$

Since  $\theta$  is distributed normally with zero mean value, its mean absolute value is related to its standard deviation  $\sigma_\theta$  as

$$\langle |\theta| \rangle = (2/\pi)^{0.5} \sigma_\theta = (2/\pi)^{0.5} \langle \theta^2 \rangle^{0.5}. \quad (12)$$

Based on (11) and (12), one can assume:

$$\sigma_\theta^2 \approx (\pi/2)^2 \sigma_\alpha^2. \quad (13)$$

The standard deviation  $\sigma_\theta$  is the parameter that describes the magnitude of crystal flutter, although the radar polarimetric parameters depend primarily on  $\alpha$  and not directly on  $\theta$ . Combining (9) and (13) and knowing that for the zero mean value  $\sigma_\alpha^2 = \langle \alpha^2 \rangle$ ,  $\sigma_\theta$  can be expressed in terms of the ratio  $H_{\text{LDR}}/S_{\text{LDR}}$  as

$$\sigma_\theta \approx 0.9 \langle (H_{\text{LDR}}/S_{\text{LDR}}) \rangle^{0.5}. \quad (14)$$

Allowing that most dendritic crystals grow rapidly to sizes large enough to introduce some secondary motions and thus assuming that flutter does not depend on crystal diameters, (14) can potentially be used for estimating standard deviations of the dendrites vertical axes from the vertical direction for particle populations. Note that depolarization ratios in (14) are for small radar elevation angles ( $\chi < 5^\circ$ ), and they are referred to a perfect radar hardware (i.e., negligible polarization cross talk and the perfect horizontal-vertical and slant-45° linear polarization bases). If flutter does depend on crystal diameters, estimates from (14) will be applicable to the particles that contribute most to the radar signals. It should be emphasized that the above derivations include the underlying assumption that flutter is small so that  $\tan(\alpha) \approx \sin(\alpha) \approx \alpha$ ,  $\cos(\alpha) \approx 1$ , and the same relations are valid for  $\theta$  when the angles are in radians. The above approximations become progressively less valid when  $\alpha$  and  $\theta$  increase beyond about  $10^\circ$ , and (14) is expected to become biased to higher values under these conditions.

Equation (14), obtained here independently for estimating  $\sigma_\theta$ , is closely related to the estimator suggested earlier by Hendry et al. (1987) for  $\sigma_\alpha$  in raindrop angular distributions:

$$(K_{22})_{\text{max}}/(K_{22})_{\text{min}} = (1 + \rho_4)/(1 - \rho_4), \quad (15)$$

where  $\rho_4 = \exp(-8\sigma_\alpha^2)$ , and  $(K_{22})_{\text{max}}$  and  $(K_{22})_{\text{min}}$  are the maximum and minimum return powers on the cross-linear polarization when the transmitted linear polarization is rotated with respect to the horizontal. For hydrometeors with the preferential horizontal ori-

entation, the minimum and maximum cross-linear polarization powers are observed when the horizontal-vertical and the slant 45°–135° polarization bases are used, respectively. For the dendritic crystals considered here,

$$(K_{22})_{\text{max}}/(K_{22})_{\text{min}} \approx (S_{\text{LDR}}/H_{\text{LDR}})k(\alpha). \quad (16)$$

For small values of  $\sigma_\alpha$ , and assuming the relations between  $\alpha$  and  $\theta$  discussed above, the combination of (15) and (16) can be expressed in the form of (14). When the measurements of  $H_{\text{LDR}}$  and  $S_{\text{LDR}}$  are separated in time, as in the experimental data shown below, for estimations of the flutter standard deviation it is better to use the ratio  $H_{\text{LDR}}/S_{\text{LDR}}$  rather than the ratio  $(K_{22})_{\text{min}}/(K_{22})_{\text{max}}$  since the estimates using the latter ratio assume that not only scatterer habits but also scatterer concentrations do not change.

It can also be shown (e.g., Matrosov et al. 2001) that SLDR for horizontally oriented crystals is equivalent to the circular depolarization ratio (CDR), which is defined as the ratio of the copolar and cross-polar radar returns when circularly polarized radar signals are transmitted. With the assumption that flutter is small, this essentially means that SLDR in (7), (9), and (14) can be substituted for CDR. The analysis in this study, however, is made for SLDR since no CDR measurements were performed during MWISP. Making CDR measurements with the NOAA  $K_a$ -band radar requires installing a different PRP, while switching between SLDR and HLDR requires only rotating the same PRP to different angles with respect to the horizontal.

### 3. Experimental example

Figure 3 shows an example of depolarization measurements taken by the NOAA  $K_a$ -band radar on 14 April 1999 during MWISP in a shallow weakly precipitating winter storm consisting mostly of single pristine dendrites. Radar reflectivities observed during this observation period were in the  $-6$  to  $+6$  dBZ range; (Fig. 4b in Reinking et al. 2002). A pair of over-the-top (vertical plane) range-height indicator (RHI) radar scans in the  $87^\circ$  azimuth direction present SLDR (Fig. 3a) and HLDR (Fig. 3b) measurements that are closely separated in time. The radar elevation angles lower than  $\chi < 18^\circ$  were partially blocked by Mt. Washington. Propagation effects tend to increase both HLDR and SLDR as the radar signals propagate through a medium of nonspherical hydrometeors. For short observational ranges used in MWISP, however, these effects do not exceed a few tenths of 1 dB (Matrosov et al. 2001). The ratio  $H_{\text{LDR}}/S_{\text{LDR}}$  will be affected even less by propagation effects than individual depolarization ratios, so these effects can be ignored for the considered experimental example.

Values of HLDR and SLDR measured experimentally with the NOAA ETL  $K_a$ -band radar are not pure

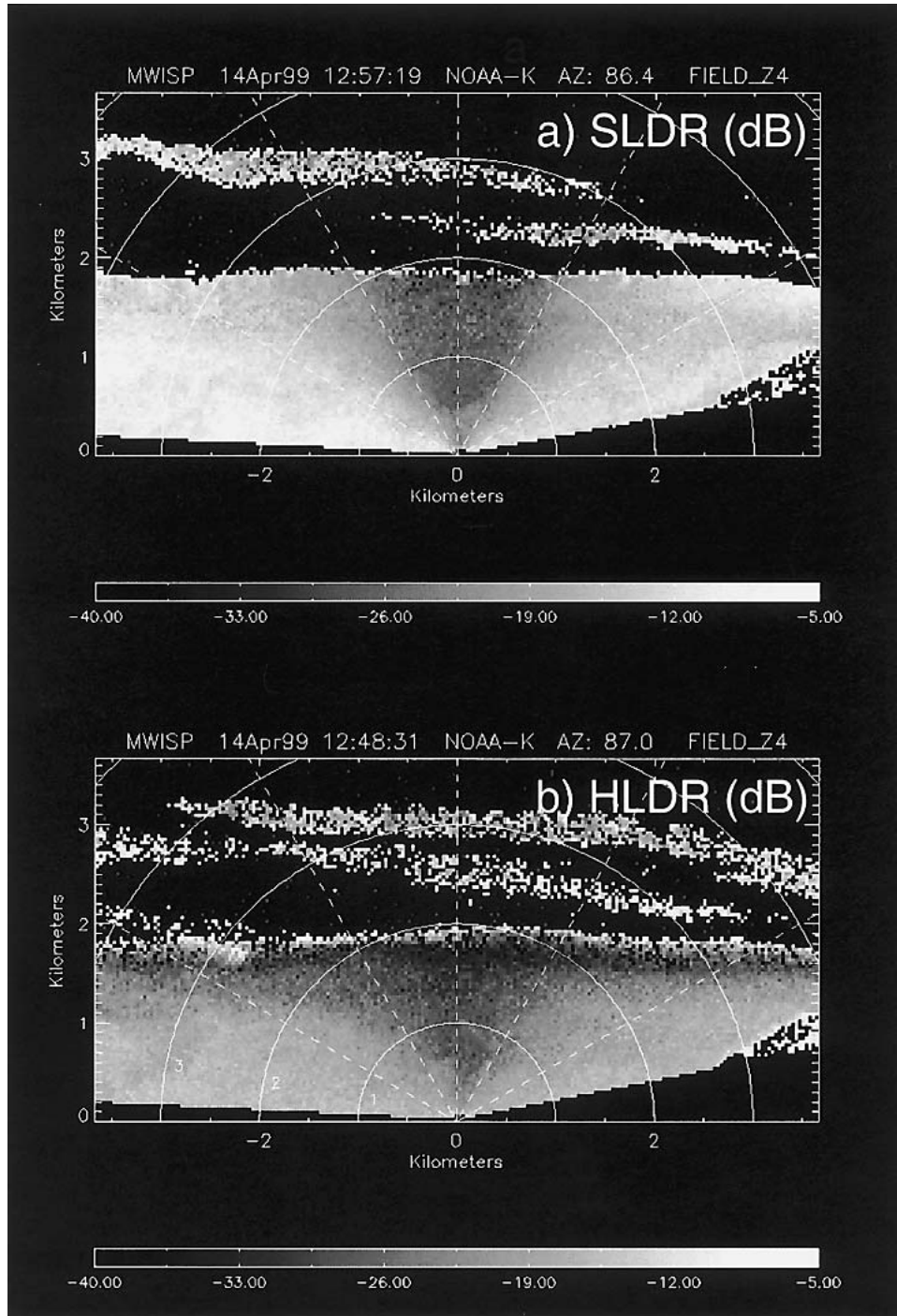


FIG. 3. RHI images of (a) SLDR at 1257 UTC 14 Apr 1999 and (b) HLDR at 1249 UTC 14 Apr 1999 during MWISP.

due to three factors: (a) the radar polarization cross talk limit of about  $-35$  dB, (b) the  $177.4^\circ$  rather than  $180^\circ$  degree phase shift of the PRP, and (c) an imperfect alignment of the PRP. These factors cause the transmitted polarizations to be imperfect for both the slant  $-45^\circ$  linear base (for SLDR measurements) and the

horizontal-vertical base (for HLDR measurements). Imperfection of this kind is not unusual for meteorological radars. For many other radars, the polarization imperfections are usually ignored, but special calibration procedures during measurements in drizzle (Matrosov et al. 2001; Reinking et al. 2002) were used to

establish real polarizations employed by the NOAA ETL  $K_a$ -band radar during MWISP.

In Fig. 3, the Mt. Washington observatory is located along the elevation direction  $\chi \approx 18^\circ$  at an altitude of about 1.2 km above the radar site. Particle sampling at the radar and observatory site elevations during the described weather event indicated that the diameters of the dendrites were nominally  $2 \pm 1$  mm. The observer electronic logbook in the radar included the following record at the time of the radar sampling used here (1257 UTC) when the dendrites were pristine: "Strong signatures of planar crystals in both slant and horizontal modes, with distinct differences between the two polarizations; . . . sampled clean [unrimed] dendrites on black velvet with a rare rimed one." The next record of crystals sampled during several minutes ending at 1327 UTC notes photographs taken of "dendrites, some clean, some with more riming than a half hour ago, some as large as 3 mm." An example of a dendrite photograph from this event is shown in Fig. 4. More photographs of dendrites from this case are presented by Reinking et al. (2002). To summarize, the crystal observations indicate pristine dendrites with typical sizes of about 2 mm at the time of the radar measurements. The possible simultaneous presence of some amount of pristine hexagonal plates cannot be ruled out, although the dendrites, being considerably larger than the plates, would have dominated the radar echoes by several orders of magnitude.

Figure 5 presents elevation angle dependencies of both HLDR and SLDR at fixed altitudes of 1.4 and 1.2 km above the radar site, characterizing the layer of dendrites at these altitudes. The measurements are somewhat noisy, indicating the fluctuating nature of the radar signals. The SLDR data for a given  $\chi$  are generally not as noisy as HLDR data which, in part, is due to a stronger cross-polar component of the radar returns in SLDR. Given the measurement noise, the SLDR and HLDR elevation angle patterns at 1.4 and 1.2 km are essentially identical indicating the closeness orientation and habits patterns at these two altitudes. The experimental depolarization values in Fig. 5 are plotted only for data points when radar echoes were 3 dB above the receiver noise. As a result of this thresholding, data in Fig. 5b have smaller elevation angle coverage, while in Fig. 5a, good data are shown down to elevation angles near  $15^\circ$  at both sides of the scans.

The depolarization elevation angle patterns in Fig. 5



FIG. 4. A photograph of sampled 1–2-mm dendrites, taken during the discussed event.

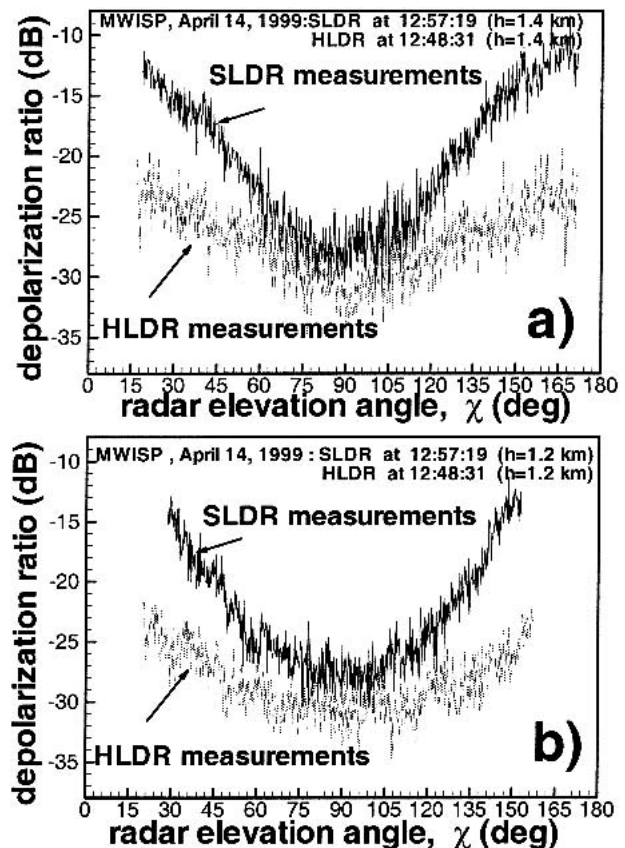


FIG. 5. SLDR at 1257 UTC 14 Apr 1999 and HLDR at 1249 UTC 14 Apr 1999 as a function of the radar elevation angle as measured in the layer of single pristine dendrites at (a) 1.4 km and (b) 1.2 km above ground during MWISP.

are clearly indicative of dendrite crystals. As shown by Matrosov et al. (2001), depolarization measurements for such crystals exhibit a large dynamic range in SLDR values which monotonically increase from minimums near the vertical (zenith) incidence to values around  $-11$ – $-13$  dB at low elevations. SLDR values are least prone to flutter at  $\chi \approx 45^\circ$  and, at this angle, pristine dendrites exhibit SLDR  $\approx -20$  dB as opposed to SLDR  $\approx -28$  dB at near vertical incidence for the MWISP configuration of the NOAA ETL  $K_a$ -band radar. Riming and aggregation reduce SLDR values at  $\chi \approx 45^\circ$ .

A distinct difference between HLDR and SLDR patterns with changing elevation angle can be seen. This difference is attributed to the preferential orientation effects because, for the random orientation of crystals, SLDR and HLDR should be identical. HLDR values are smaller than SLDR values, and the dynamic range of SLDR is significantly larger than that of HLDR. The patterns of depolarization measurements are quite symmetrical relative to  $\chi = 90^\circ$ , which indicates homogeneity of the dendrite layer.

Rotating PRP and observing the magnitude of the

copolar return as a function of the PRP rotation angle when measurements are taken at a fixed elevation angle allows one to determine the mean value of  $\alpha$  (Matrosov et al. 2001). The measurements with a rotating PRP at several fixed values of  $\chi$  (not shown) indicated that the mean value of  $\alpha$  and, hence, the mean value of  $\theta$  were essentially zero, so the value of  $\sigma_\theta$  was a sole parameter characterizing crystal orientation. The lowest radar elevations, with reliable estimates of both HLDR and SLDR, were near  $\chi = 15^\circ$  and  $\chi = 165^\circ$  (see Fig. 5). The  $165^\circ$  estimates correspond to the elevation  $\chi = 180^\circ - 165^\circ = 15^\circ$  on the opposite side.

It was shown (Matrosov et al. 2001) and also seen from Fig. 6 that both SLDR and HLDR change very little (typically within 0.5 dB for SLDR and 0.2 dB for HLDR) in the elevation angle range  $0^\circ$ – $15^\circ$ , so the use of measurements at  $\chi = 165^\circ$  or  $\chi = 15^\circ$  as a proxy for measurements at  $\chi = 0^\circ$  or at  $\chi = 180^\circ$  is generally justified given the measurement noise. For better flutter retrievals in this study, however, the values of  $H_{LDR}$  and  $S_{LDR}$  observed at  $15^\circ$  off horizontal were corrected by 0.5 dB (for SLDR) and 0.2 dB (for HLDR) to get their estimates at near horizontal viewing. Using these slightly corrected  $H_{LDR}$  and  $S_{LDR}$  values in (14) results an  $\sigma_\theta$  estimate of about  $12^\circ$ .

#### 4. Estimation of crystal flutter by matching theoretical and experimental data

The derivation of Eq. (14) involved a number of assumptions concerning the extent of flutter and the relative magnitude of the backscattering amplitudes  $S_h$  and  $S_v$ ; most importantly, (14) is applicable to the depolarization ratios in the perfect horizontal–vertical (for HLDR) and the perfect slant- $45^\circ$  linear (for SLDR) bases. This equation, although quite convenient, does not provide a direct estimate of the uncertainties in-

involved when making flutter estimates. Another approach of getting an estimate of  $\sigma_\theta$  is to try to calculate theoretically the depolarization ratios as a function of the radar elevation angle  $\chi$  and to compare the results of calculations and measurements for different values of flutter (i.e., different values of  $\sigma_\theta$ ). With such calculations, there is no need to make assumptions that flutter is small, that the ratio of the amplitudes  $S_h$  and  $S_v$  is fixed, or that the radar cross talk is negligible. The actual polarization states can be considered by accounting for the parameters of the particular PRP (Matrosov et al. 2001). An additional criterion, the depolarization dependence on  $\chi$ , can be used to judge how appropriate the flutter estimates are for a particular crystal type.

The calculations of HLDR and SLDR for the particular PRP characteristics (i.e., for the real polarization bases used in MWISP) and the  $-35$ -dB radar polarization cross talk were performed for a distribution of pristine dendrites modeled by the first-order gamma function with a model diameter  $D_o = 2$  mm. This function was shown to be appropriate for describing the size distributions of ice hydrometeors (Mazin and Khrgian 1989). The computational algorithm for depolarization ratios is presented in detail by Matrosov (1991) and Matrosov et al. (2001). Figure 6 shows the results of the depolarization calculations for  $\sigma_\theta = 3^\circ, 9^\circ,$  and  $15^\circ$ . In order to show the sensitivity of depolarization ratios to the choice of  $D_o$ , results for  $D_o = 1.5$  mm and  $\sigma_\theta = 3^\circ$  are also shown in this figure. It can be seen that the variability of HLDR and SLDR with  $D_o$  in this range is rather small. The increase of  $D_o$  causes the particle to be more oblate, which increases depolarization. On the other hand, larger particles have smaller refractive indices (i.e., they are optically “softer”) than smaller particles, and hence, they cause less depolarization compared to scatterers of the same oblateness but with a larger refractive index. This mechanism partially balances the increase in depolarization caused by the increase of the average oblateness, so the resulting effect is rather small. For  $D_o = 2$  mm and  $\sigma_\theta = 9^\circ$ , HLDR calculated for the perfect horizontal–vertical polarization basis and SLDR calculated for the perfect slant- $45^\circ$  polarization basis are also shown in Fig. 6 for reference.

It can also be seen from Fig. 6 that variability of SLDR due to crystal flutter (i.e., due to  $\sigma_\theta$ ) is significantly less than that of HLDR, especially for  $\chi < 60^\circ$  and  $\chi > 120^\circ$ . As mentioned before, this variability in SLDR is almost nonexistent at  $\chi \approx 45^\circ$  (and  $\chi \approx 135^\circ$ ). Measurements of SLDR at these radar elevation angles can be used for determining particle shapes since orientation effects here are minimal. Effects of the “imperfections” of the used polarizations are also small near these values of  $\chi$ . In more detail, the method for estimating hydrometer shapes that uses SLDR measurements near  $\chi \approx 45^\circ$  is described by Matrosov et al. (2001).

Figure 7 presents depolarization measurements at the 1.4-km altitude superimposed by modeled data calculated for  $\sigma_\theta = 9^\circ \pm 3^\circ$ . The 1.4-km data (Fig. 5a) are

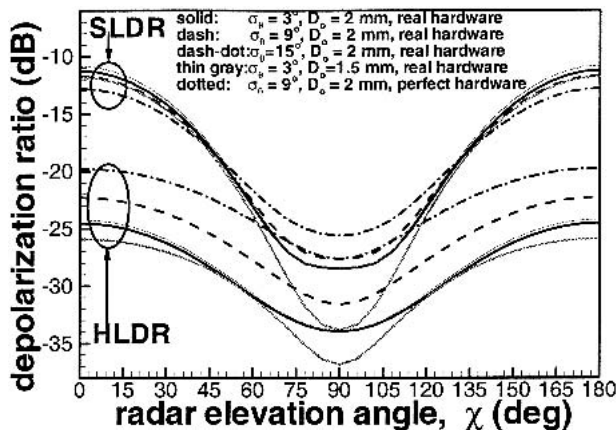


FIG. 6. Results of modeling of SLDR and HLDR as a function of radar elevation angle for pristine dendrites for several values of the standard deviation of flutter  $\sigma_\theta$  and the characteristic dendrite diameter  $D_o$ .

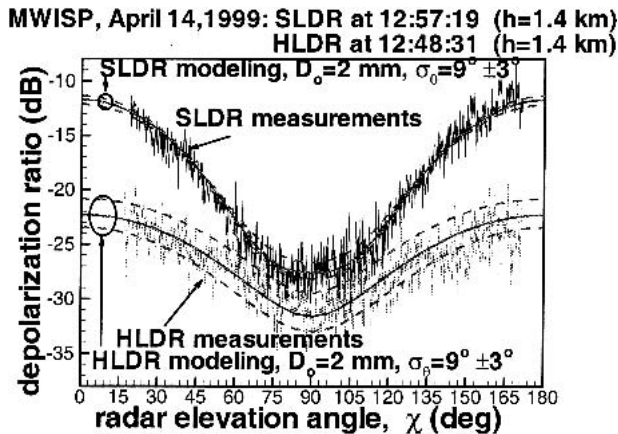


FIG. 7. Measurements of SLDR and HLDR from Fig. 5 with superimposed results of calculations with  $\sigma_\theta = 9^\circ \pm 3^\circ$  and  $D_0 = 2$  mm.

chosen rather than 1.2-km data (Fig. 5b) because of larger elevation angle coverage. The elevation angle patterns of depolarization at these two altitudes are very similar, indicating very close flutter and habit properties at these altitudes, so this choice does not compromise the results.

In Fig. 7, The calculations effectively bracket the measurements, especially for HLDR, which is significantly more sensitive to crystal flutter than SLDR. The results presented in Fig. 6 can be considered as an estimate of  $\sigma_\theta$  with its uncertainties. The theoretical estimate obtained from (14) using experimental HLDR and SLDR data,  $\sigma_\theta \approx 12^\circ$ , is on the high end of the estimate from matching the measurements and model calculations. This is an encouraging fact indicating that the magnitude of flutter and imperfections in the polarizations used in the radar configuration during MWISP are not very significant. Therefore, the estimate from the approximate analytical equation (14) using observed depolarizations is not much different from the careful estimate using the matching procedure. Note also that, if the calculated values of HLDR ( $\sim -26$  dB) and SLDR ( $\sim -11.7$  dB) in perfect polarization bases for  $\sigma_\theta = 9^\circ$  and  $\chi = 0^\circ$  (see Fig. 5) rather than observed HLDR and SLDR, are substituted in (14), they provide an estimate of  $\sigma_\theta \approx 10^\circ$  that is quite close to the matching result of  $\sigma_\theta = 9^\circ \pm 3^\circ$ . Given the arguments expressed above, the matching estimate,  $\sigma_\theta = 9^\circ \pm 3^\circ$ , should be considered meaningful and in general agreement with the estimate from the approximate analytical equation (14).

It should be mentioned that the matching theoretical curves in Figs. 6 and 7 were calculated using the assumptions about dendrite aspect ratio and density from (4) and (5). An  $\sim 15\%$  uncertainty in these assumptions can cause the variability of the theoretical curves by as much as 1 dB. Such variability values are still less than the depolarization measurement error and this will not

significantly change the flutter estimates given a relatively high degree of their uncertainty ( $\pm 3^\circ$ ). Besides, the assumptions (4) and (5) were shown to be appropriate since their use results in good agreement between theoretical calculations and measurements of radar parameters of dendrites with a variety polarization states and in different field experiments (Matrosov et al. 1996, 2001).

Furthermore, the estimates from the depolarization measurements are in keeping with other, independent estimates of flutter. Mallman et al. (1980) showed both photographic and theoretical evidence of narrow sun pillars due to plate crystals with “nearly” horizontal orientations (e.g.,  $\sigma_\theta \approx 2^\circ$ ) and broader sun pillars due to less horizontal orientations (e.g.,  $\sigma_\theta \approx 10^\circ$ ). Comparable flutter is exhibited also by columnar crystals, although there were no combined HLDR and SLDR measurements in columnar crystals during MWISP. Photogrammetric measurements of Kajikawa (1976) indicated canting angles, or flutter, of  $10^\circ$ – $25^\circ$ . Zikmunda and Vali (1972) found that, for individual rimed columnar crystals, about 40% fell with less than a  $5^\circ$  cant and about 90% fell with less than a  $15^\circ$  cant, but the canting was as large as  $75^\circ$  for a few crystals. The riming tended to induce imbalances to increase secondary settling motions over those of pristine crystals. The samples for some of these analyses are small, and the depolarization measurements can potentially provide a better representation of the flutter of large crystal populations.

Typical values for the Reynolds numbers for observed crystals can be estimated. The fall velocities of dendritic crystals as a function of their diameters are largely available from the literature. Dendrites with diameters of about 1–2 mm, as observed in the analyzed cases, are characterized by fall velocities between about 30 and 60  $\text{cm s}^{-1}$  (Heymsfield 1972; Pruppacher and Klett 1997; Sassen 1980). The fall velocities of observed crystals can also be roughly estimated from Doppler velocity measurements with the radar beam pointing vertically,  $V_D$ . Values of  $V_D$  at vertical incidence represent the sum of the vertical air motions,  $V_a$ , and the reflectivity-weighted crystal fall velocities,  $V_r$ . Figure 8 shows measurements of  $V_D$  at different altitudes at the moments when the radar beam was pointed within  $0.25^\circ$  from the vertical direction. The presented measurements cover the period from 1210 to 1310 UTC when the precipitating cloud consisted mostly of pristine dendrites. The mean value of  $V_D$  is about 50  $\text{cm s}^{-1}$ . This value can be considered as an estimate of hydrometeor fall velocities assuming that the contribution from  $V_a$ , which represents updrafts and downdrafts, largely cancels out as a result of averaging. The spread of  $V_D$  around its mean value in Fig. 8 is due to variability in  $V_r$  and, probably most importantly, due to individual updraft and downdraft in air motions at a particular measurement time. This radar-estimated mean value of  $V_r$  of 50  $\text{cm s}^{-1}$  is in agreement with data from the literature referenced above.



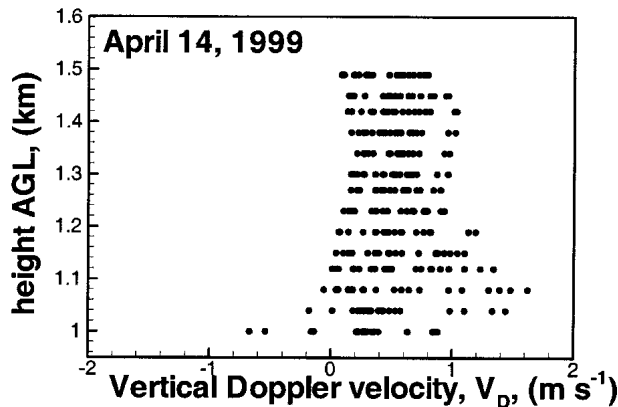


FIG. 8. Measurements of Doppler velocities at vertical incidence between 1209 and 1309 UTC.

Summarizing the size and fall velocity information given above, one can conclude that for a kinematic viscosity of  $0.12 \text{ cm}^2 \text{ s}^{-1}$  at the altitude of the observed layer, the typical values of  $N_{\text{Re}}$  for such dendrites were usually in a range of about 40–100. Thus, values of  $N_{\text{Re}}$  for the observed crystals and the fact that they demonstrated measurable flutter are in accord with Kajikawa's (1992) estimate that natural planar crystals begin to exhibit secondary motions if  $N_{\text{Re}} \geq 40$ . Here  $N_{\text{Re}}$  for occasional 3-mm dendrites could exceed 100.

## 5. Conclusions

An approach has been suggested and applied for deducing the magnitude of secondary motion, or “flutter,” of falling planar ice crystals around their preferred horizontal orientation. This approach is based on combined measurements of radar depolarization ratios in the traditional horizontal-vertical basis (HLDR) and in the basis rotated to a  $45^\circ$  slant with respect to the horizontal (SLDR). This approach can also be applied to the combination of HLDR and circular depolarization ratio (CDR) measurements since SLDR and CDR are essentially identical for horizontally oriented planar crystals. The analyses, however, were performed for an HLDR and SLDR pair, since no CDR measurements were made during MWISP.

The suggested approach is applicable to situations when one single planar hydrometeor habit dominates radar returns, which happens, for example, in winter boundary-layer snow clouds with weakly precipitating dendrites when aggregation and riming is small. Higher ice clouds usually contain a variety of habits including many irregular shapes and usually do not provide clear depolarization patterns as a function of radar elevation angle. In addition to that, depolarization measurements in higher clouds are hampered by the radar sensitivity issues due to requirements for measurements of very weak echoes in one of the receiving polarization chan-

nels. The suggested approach can potentially be extended for prolate shape cloud particles (e.g., columns, bullets, needles), although it is beyond the scope of the current study, in part, due to the lack of experimental radar data for clouds where columnar hydrometers were the dominant hydrometeor habit.

The difference in sensitivities of HLDR and SLDR to the crystal orientation provides a basis for quantitative estimation of the angular standard deviation  $\sigma_\theta$  of dendrite axes of rotation from a vertical direction. An analytical expression was suggested to estimate  $\sigma_\theta$  from the ratio  $H_{\text{LDR}}/S_{\text{LDR}}$  at low radar elevation angles for small flutter. This expression is applicable to the depolarization ratios measured for perfect horizontal-vertical and the perfect slant  $-45^\circ$ – $135^\circ$  linear polarizations. Another approach to estimate  $\sigma_\theta$  is by matching observed and theoretical dependencies of HLDR and SLDR as functions of radar elevation angle. This matching does not require crystal flutter to be small, it is not limited to low radar elevation angles, and it considers real polarization states rather than perfect ones, which are rarely achievable.

The suggested depolarization approach was applied to a case from the MWISP field experiment when a weakly precipitating winter storm producing single pristine dendrites was monitored with the NOAA ETL polarimetric  $K_a$ -band radar. The typical observed dendrites were characterized by the Reynolds numbers  $N_{\text{Re}}$  of about 40–100, which suggests stable fall attitudes for perfectly symmetrical crystals and initiation of secondary motions for actual, less symmetrical crystals. An estimate of  $\sigma_\theta$  from the analytical expression using the ratio of observed HLDR and SLDR values was about  $12^\circ$ , which is at the high end of more robust estimates from matching the theoretical and experimental HLDR and SLDR radar elevation angle patterns that provided  $\sigma_\theta = 9^\circ \pm 3^\circ$ . This general agreement indicates that the magnitudes of crystal flutter and “imperfections” in the polarization bases actually used were small enough for the analytical expression to provide a meaningful result. Although the matching procedure is generally more robust since it accounts for the real polarization states and the polarization “cross talk,” the value of the analytical derivation of the equation is in displaying the physical mechanisms that are responsible for unraveling the crystal shape and orientation effects.

The experimental case of 14 April 1999 was characteristic of several weakly precipitating pristine dendrite cases observed during MWISP. The other cases exhibited very similar elevation angle patterns and magnitudes of HLDR and SLDR. The sizes of the sampled crystals were also generally the same and were characteristic of those normally attained by dendrites.

Crystal flutter may be caused not only by eddy shedding but also by turbulent air motions (e.g., Sassen 1980), so the approach suggested here, to estimate the magnitude of flutter, might be used for studies of turbulence effects on crystal falling attitudes when inde-

pendent information on turbulence is available. Other important implications of this approach are concerned with the lidar remote sensing of ice clouds due to the significance of the specular reflection effect, initiation of precipitation, radar-based icing detection algorithms, and ice cloud radiative modeling where assumptions about particle orientation influence the magnitude of the cloud radiative effect. Collectively, measurements from various sources and methods show that the deviations of the settling orientation from horizontal may frequently be small but may vary. Thus, it is advantageous to have a means to estimate degree of flutter as provided by the depolarization approach.

*Acknowledgments.* The MWISP experiment and a part of this research was funded by the Aviation Weather Research Program of the Federal Aviation Administration (FAA). The views expressed are those of the authors and do not necessarily represent the official policy of the FAA.

#### REFERENCES

- Bohren, C. F., and D. R. Huffman, 1983: *Absorption and Scattering of Light by Small Particles*. John Wiley and Sons, 530 pp.
- Dungey, C. E., and C. F. Bohren, 1993: Backscattering by non-spherical hydrometeors as calculated by the coupled-dipole method: An application in radar meteorology. *J. Atmos. Oceanic Technol.*, **10**, 526–532.
- Hendry, A., Y. M. M. Antar, and G. C. McCormic, 1987: On the relationship between the degree of preferred orientation in precipitation and dual-polarization radar echo characteristics. *Radio Sci.*, **22**, 37–50.
- Heymsfield, A. J., 1972: Ice crystal terminal velocities. *J. Atmos. Sci.*, **29**, 1348–1357.
- Holt, A. R., 1984: Some factors affecting the remote sensing of rain by polarization diversity radar in 3- to 35-GHz frequency range. *Radio Sci.*, **47**, 1399–1421.
- Kajikawa, M., 1976: Observation of falling motion of columnar snow crystals. *J. Meteor. Soc. Japan*, **54**, 276–283.
- , 1992: Observations of the falling motion of plate-like snow crystals, Part I: The free-fall patterns and velocity variations of unrimed crystals. *J. Meteor. Soc. Japan*, **70**, 1–9.
- Korolev, A. V., G. A. Isaac, and J. Hallet, 2000: Ice particle habits in stratiform clouds. *Quart. J. Roy. Meteor. Soc.*, **126**, 2873–2902.
- Mallman, A. J., J. L. Hock, and R. G. Greenler, 1980: Comparison of sun pillar with light pillars from nearby light sources. *Appl. Opt.*, **37**, 1441–1449.
- Matrosov, S. Y., 1991: Theoretical study of radar polarization parameters obtained from cirrus clouds. *J. Atmos. Sci.*, **48**, 1062–1070.
- , 1992: Radar reflectivity in snowfall. *IEEE Trans. Geosci. Remote Sens.*, **30**, 454–461.
- , and R. A. Kropfli, 1993: Cirrus cloud studies with elliptically polarized Ka-band radar signals: A suggested approach. *J. Atmos. Oceanic Technol.*, **10**, 684–692.
- , R. F. Reinking, R. A. Kropfli, and B. W. Bartram, 1996: Estimations of ice hydrometeor types and shapes from radar polarization measurements. *J. Atmos. Oceanic Technol.*, **13**, 85–96.
- , —, —, B. E. Martner, and B. W. Bartram, 2001: On the use of radar depolarization ratios for estimating shapes of ice hydrometeors in winter clouds. *J. Appl. Meteor.*, **40**, 479–490.
- Mazin, I. P., and A. K. Khrgian, Eds., 1989: *Clouds and Cloudy Atmosphere*. Gidrometeoizdat, 648 pp.
- Platt, C. M. R., 1978: Lidar backscattering from horizontal ice crystal plates. *J. Appl. Meteor.*, **17**, 482–488.
- Pruppacher, H. R., and J. D. Klett, 1997: *Microphysics of Clouds and Precipitation*. Kluwer Academic, 954 pp.
- Reinking, R. F., S. Y. Matrosov, R. A. Kropfli, and B. W. Bartram, 2002: Evaluation of a 45° slant quasi-linear radar polarization state for distinguishing drizzle droplets, pristine ice crystals, and less regular ice particles. *J. Atmos. Oceanic Technol.*, **19**, 296–321.
- Ryerson, C. C., M. K. Politovich, K. L. Rancourt, G. G. Koenig, and R. F. Reinking, 2000: Mt. Washington Icing Sensors Project: Conduct and preliminary results. *Proc. 38th AAIA Aerospace Science Meeting and Exhibit*, Paper No. AAIA-2000-0488, Reno, NV, AIAA, 10 pp.
- Sassen, K., 1980: Remote sensing of planar ice crystal fall attitudes. *J. Meteor. Soc. Japan*, **58**, 422–429.
- Zikmunda, J., and G. Vali, 1972: Fall patterns and fall velocities of rimed ice crystals. *J. Atmos. Sci.*, **29**, 1334–1347.